

# Superconductivity and Charge Density Wave in a Quasi-One-Dimensional Spin Gap System

Sam T. Carr<sup>1,2</sup> and Alexei M. Tsvelik<sup>1</sup>

<sup>1</sup>*Department of Physics, Brookhaven National Laboratory, Upton NY 11973, USA*

<sup>2</sup>*Department of Theoretical Physics, Oxford University, 1 Keble Road, Oxford, UK*  
(December 2, 2024)

We consider a model of spin-gapped chains weakly coupled by Josephson and Coulomb interactions. Combining such non-perturbative methods as bosonization and Bethe ansatz to treat the intra-chain interactions with the Random Phase Approximation for the inter-chain couplings and the first corrections to this, we investigate the phase diagram of this model. The phase diagram shows both charge density wave ordering and superconductivity. These phases are separated by line of critical points which exhibits an approximate an  $SU(2)$  symmetry. We consider the effects of a magnetic field on the system. We apply the theory to the material  $Sr_2Ca_{12}Cu_{24}O_{41}$  and suggest further experiments.

PACS numbers: 71.10.Hf, 74.20.Mn

## I. INTRODUCTION

Quasi-one-dimensional (1D) models are often used to test various theoretical ideas in the area of strongly correlated electron systems for the simple reason that most known non-perturbative approaches work only in one dimension.<sup>1,2</sup> The route often taken is to use a non-perturbative solution of a strictly one-dimensional model and then use mean field or the Random Phase Approximation (RPA) to take into account the inter-chain interactions. Through techniques such as bosonization and Bethe ansatz, many results are known about such one-dimensional systems as spin chains and Tomonaga-Luttinger liquids which form the skeleton of these quasi-one-dimensional models. Linking these using the RPA formalism has yielded many successful experimental predictions, for example for linear conductors<sup>3</sup> and for magnetic systems.<sup>4-6</sup>

As it is well known, the RPA represents the leading term in a perturbation expansion in  $1/z_{\perp}$ , where  $z_{\perp}$  is the number of nearest-neighbour chains in the lattice. Since for real systems this number is not large, it is important to know about higher order contributions in  $1/z_{\perp}$ . The recent results for the quasi-one-dimensional Heisenberg magnets indicate that the next-to-leading  $1/z_{\perp}$ -corrections are numerically small leading to a slight shift in the transition temperature.<sup>7,8</sup>

In this paper we follow the same road and discuss a simple model of a non-BCS superconductor. In the model we consider the formation of superconducting pairs on one-dimensional chains is triggered by formation of a spin gap. The three-dimensional coherence is established through the inter-chain Josephson coupling. Since the latter coupling competes with the Coulomb interaction, which can destroy the superconductivity and establish Charge Density Wave (CDW) ordering. As we shall show, these two phases are separated by a critical line with increased symmetry. Near this line, we take into account the interplay between these two interactions considering corrections to RPA.

The model we use has been considered in some detail recently<sup>9</sup> in the context of high- $T_c$  superconductivity. It was assumed that the one-dimensional behaviour came about from the formation of stripes.<sup>10</sup> Since in the stripe picture, fluctuations of the stripes dephase the CDW coupling,<sup>11</sup> only the SC inter-chain interaction was considered. In our paper we retain the Coulomb interaction and therefore expect it to be relevant to materials that are structurally quasi-one-dimensional such as the Bechgaard salts or some cuprate materials such as the family  $Sr_{12-x}Ca_xCu_{24}O_{41}$ .

In section II we introduce the model we will be dealing with. In section III we show that this model has an  $SU(2)$  symmetric quantum critical line. In section IV we calculate the transition temperature for the model within the RPA approximation. Treating the inter-chain coupling in the mean field approximation we obtain an effective sine-Gordon model for each chain. Using the exact results for this model we calculate the zero temperature spectral gap  $M$  and derive the expression for the ratio  $T_c/M$ . Here, we also consider the properties of our system in a magnetic field. In section V we look at the first corrections to RPA which gives us an improved phase diagram of the model. In section VI we show that the same general behaviour also occurs in two dimensions, although the transition here is Kosterlitz-Thouless rather than the symmetry breaking found in higher dimensions. Finally, in section VII, we show that the quasi-1D compound  $Sr_2Ca_{12}Cu_{24}O_{41}$  is a beautiful example of our model and we discuss the measured properties of it in relation to our theory. We also make some quantitative predictions about this material which could be confirmed by further experiments.

## II. THE MODEL

Let us consider a system of conducting one-dimensional units (we will call them *chains*, though in reality they may be, for instance, ladders) weakly coupled to each other. We assume that filling of each individual chain is incommensurate with the lattice and the dominant interaction is such that a gap opens in the spin sector. In a specific case of single chains the realistic description of the spin sector is given by the SU(2) Thirring model Hamiltonian<sup>1</sup>. The Hamiltonian density is

$$\mathcal{H}_{\text{chain}} = \mathcal{H}_{\text{charge}} + \mathcal{H}_{\text{spin}}, \quad (1)$$

$$\mathcal{H}_{\text{charge}} = \frac{1}{2}[K_c(\partial_x\Theta)^2 + K_c^{-1}(\partial_x\Phi)^2] \quad (2)$$

where  $[\Theta(x), \Phi(y)] = i\theta(x-y)$ . In a specific case of single chains the realistic description of the spin sector is given by the SU(2) Thirring model Hamiltonian:<sup>1</sup>

$$\mathcal{H}_{\text{spin}} = \frac{2\pi v_s}{3}(: J^a J^a : + : \bar{J}^a \bar{J}^a :) - g : J^a \bar{J}^a : \quad (3)$$

where  $v_s$  is the spin velocity and  $J^a, \bar{J}^a$  are chiral SU(2) currents satisfying the level  $k=1$  SU(2) Kac-Moody algebra. The spin gap is generated when  $g > 0$  such that the current-current interaction in the spin sector is marginally *relevant*. In the case of ladders a description of the spin sector is more complicated; this however does not affect the charge Hamiltonian and therefore will not concern us here.

Whatever is the mechanism of the spin gap formation, the gap blocks single-particle tunneling processes between the chains. Then the multi-particle processes generate pair hopping. In what follows we shall assume that the inter-chain tunneling matrix element is much smaller than the spin gap. In this case one can take into account only two-particle virtual processes giving rise to Josephson coupling between the chains. They lead to the following Hamiltonian

$$\mathcal{H}_{\text{sc}} = \frac{1}{2}J_{\text{eff}} \sum_{n \neq m} : \cos[\sqrt{2\pi}(\Theta_n - \Theta_m) - 2eHb_{nm}x/c] : \quad (4)$$

where the dots signify that operators are normal ordered with respect to the state with spin gap and therefore the ultraviolet cut-off for the correlation functions of bosonic exponents is  $\Delta_s$ . The fields without index are assumed to be from the charge sector, as will be the case from here on. We have also introduced external magnetic field  $H$  directed perpendicular to the chains;  $b_{nm}$  is the projection of the inter-chain lattice vector on the direction perpendicular both to the chains and the magnetic field.

An analysis of dimensionalities as shown in Appendix A yields

$$J_{\text{eff}} \sim \left(\frac{\Delta_s}{\Lambda}\right)^{1/K_c-1} \frac{t^2}{\Delta_s} \quad (5)$$

where  $t$  is the single particle hopping and  $\Lambda$  is related to the original bandwidth.

Interaction (4) has scaling dimension

$$d_{\text{sc}} = 1/(2K_c) \quad (6)$$

and therefore is relevant even for repulsive interactions in the charge sector provided they are not too strong ( $K_c > 1/2$ ). This is a well known effect of the spin gap; it generates preformed pairs making it easy for them to condense.<sup>12</sup>

There is also a Coulomb interaction between the two chains. In the spin gap regime, there is only one term in here that remains relevant: it is the coupling of  $2k_F$ -components of the charge density which gives the effective Hamiltonian density (Appendix A)

$$\mathcal{H}_{\text{cdw}} = \frac{1}{2}V_{\text{eff}} \sum_{n \neq m} : \cos[\sqrt{2\pi}(\Phi_n - \Phi_m)] : \quad (7)$$

where

$$V_{\text{eff}} \sim \left(\frac{\Delta_s}{\Lambda}\right)^{K_c} V_0. \quad (8)$$

The corresponding scaling dimension is

$$d_{\text{cdw}} = K_c/2. \quad (9)$$

The effective action for coupled chains is therefore

$$\mathcal{L}_{\text{eff}} = \frac{1}{2K_c} \sum_n (\partial_\mu \Phi_n)^2 + \frac{1}{2} \sum_{n \neq m} \{V_{nm} : \cos[\sqrt{2\pi}(\Phi_n - \Phi_m)] : + J_{nm} : \cos[\sqrt{2\pi}(\Theta_n - \Theta_m - 2eHb_{nm}x/c)] : \} \quad (10)$$

and has  $\Delta_s$  as the ultraviolet cut-off. We will be considering nearest-chain interactions only, i.e.  $V_{nm} = V, J_{nm} = J$  for neighbouring chains and zero otherwise. In what follows we will be most interested in the case  $K_c \approx 1$  when both interactions are important.

### III. AN EFFECTIVE THEORY OF THE CRITICAL POINT

For a general value of  $K_c$  the symmetry of the model is  $U(1) \times U(1)$  which corresponds to independent global shifts of  $\Phi$  and  $\Theta$ . When  $K_c = 1$  and  $V = \pm J$  the symmetry increases and becomes  $SU(2)$ . To see this we use the non-Abelian bosonization description.<sup>1,13</sup> At  $K_c = 1$  the exponents  $\exp[\pm i\sqrt{2\pi}\Phi], \exp[\pm i\sqrt{2\pi}\Theta]$  have conformal dimensions  $(1/4, 1/4)$  and can be understood as matrix elements of the tensor field  $g_{ab}$  from the  $S=1/2$  representation - the first primary field of the level  $k=1$  Wess-Zumino-Novikov-Witten model (for a discussion of this model, see e.g. Itzykson and Drouffe<sup>14</sup>):

$$\hat{g} = \begin{pmatrix} \exp[i\sqrt{2\pi}\Phi] & \exp[i\sqrt{2\pi}\Theta] \\ \exp[-i\sqrt{2\pi}\Theta] & \exp[-i\sqrt{2\pi}\Phi] \end{pmatrix}. \quad (11)$$

The Gaussian part of the action becomes the sum of the WZNW actions from individual chains:

$$\frac{1}{2} \sum_n (\partial_\mu \Phi_n)^2 \rightarrow \sum_n W[g_n]. \quad (12)$$

and the interaction term in (10) can be written as

$$L_{\text{int}} = \sum_{n \neq m} \{ (V - J) \sum_{a=1,2} [g_n^{(aa)} [g_m^+]^{(aa)} + (n \rightarrow m)] + J \text{Tr}(g_n g_m^+ + g_m g_n^+) \}. \quad (13)$$

This description is convenient since it contains only mutually local fields and therefore can be considered as the Ginzburg-Landau theory.

In three spatial dimensions the system undergoes a phase transition into the ordered state where the matrix  $g$  acquires an average value throughout the system. In the long wave limit one can replace the last term in (13) by

$$(\partial_y g)(\partial_y g^+) \quad (14)$$

and omitting the time dependence of the fields we obtain the following Ginzburg-Landau free energy:

$$F = b^{-2} \int dx d^2r \text{Tr} \left[ \frac{va_0}{16\pi} (\partial_x g^+ \partial_x g) + Jb^2 (\nabla_\perp g^+ \nabla_\perp g) \right] + F_{\text{anisotropy}} \quad (15)$$

where  $b$  is the lattice constant in the transverse direction and

$$F_{\text{anisotropy}} = (V - J)b^{-2} \int dx d^2r \sum_{a=1,2} g^{(aa)} [g^+]^{(aa)}. \quad (16)$$

We can now re-parameterize the theory. The order parameter is the  $SU(2)$  matrix  $g$ . Its relation to the CDW and SC phases  $\Theta$  and  $\Phi$  are:

$$g = \exp[i\sigma^3(\Phi + \Theta)/4] \exp[i\sigma^1\alpha/2] \exp[i\sigma^3(\Phi - \Theta)/4]. \quad (17)$$

The Ginzburg-Landau free energy density is

$$\mathcal{F} = \frac{1}{2} \rho [\cos^2(\alpha/2) (\nabla\Theta)^2 + \sin^2(\alpha/2) (\nabla\Phi)^2] + \frac{1}{2} \rho (\nabla\alpha)^2 + (V - J) \cos \alpha. \quad (18)$$

This is interpreted as follows: when  $V - J$  is positive,  $\alpha$  is pinned at  $\pi$  so that the coefficient in front of  $(\nabla\Phi)^2$  is non-zero and hence  $\Phi$ , the CDW order parameter, is constant throughout the material. When  $V - J$  is negative,  $\alpha$  is pinned at 0 and hence it is  $\Theta$ , the superconducting order parameter that acquires an expectation value. When  $V - J = 0$  we are at the critical point where the free energy of the superconducting and insulating phases becomes equal. The effects of this  $V - J$  mode will be considered throughout the rest of the paper.

#### IV. PHASE DIAGRAM IN MAGNETIC FIELD AND CRITICAL TEMPERATURE

For two chains the problem was solved by Shelton *et al.*<sup>15</sup> There are two modes; one symmetric in the two chains and the other antisymmetric. In the presence of the inter-chain interactions, the symmetric mode remains gapless and the antisymmetric sector splits into two Majorana fermions with gaps  $(V + J)$  and  $(V - J)$ .

For an infinite number of chains, we expect to see a similar sort of behaviour. The gapless symmetric mode in the case of two chains will in some sense be the Goldstone mode in our infinite system and we expect to see a range of other modes with gaps ranging from  $V - J$  to  $V + J$ . We will see that within the basic RPA approximation we cannot reproduce this behaviour: the properties will depend on the stronger of  $V$  and  $J$  but not both. However when we go beyond the first order term we can start probing the interplay between these two competing interactions.

To begin with, we estimate the critical temperature using RPA. Within this approximation the pairing and the CDW susceptibilities are given by

$$\begin{aligned}\chi_{sc} &= \frac{\chi_{sc}^{(0)}}{1 - Jz_{\perp}\chi_{sc}^{(0)}}, \\ \chi_{cdw} &= \frac{\chi_{cdw}^{(0)}}{1 - Vz_{\perp}\chi_{cdw}^{(0)}}\end{aligned}\tag{19}$$

where  $z_{\perp}$  is the number of nearest neighbour chains. These are shown diagrammatically in figure 6 (a) and (b).

When  $K_c = 1$  the bare susceptibilities are equal to each other and therefore the instability occurs in that channel where the interaction is stronger. This is shown explicitly in Appendix B. If  $K_c \neq 1$ , the instability still occurs in the stronger channel, although this now depends not only on the values of  $V$  and  $J$  but also on  $K_c$  and  $\Delta_s$ , the crossover point being

$$\left(\frac{t^2}{\Delta_s}v_c\right)^{\frac{1}{2-1/2K_c}} \sim \left(\frac{V}{v_c}\right)^{\frac{1}{2-K_c/2}}.\tag{20}$$

An important modification occurs in magnetic field which affects the inter-chain interaction in the superconducting channel (4). In this case the susceptibilities corresponding to the lattice directions  $\mathbf{l}$  should be taken at wave vector  $2e(\mathbf{H}[\hat{\mathbf{x}} \times \mathbf{l}])/c$ , where  $\hat{\mathbf{x}}$  is the unit vector along the chains. Therefore the RPA criterion for the transition is replaced by

$$1 = \sum_l J_l \chi_{sc}^{(0)} \{q = 2e(\mathbf{H}[\hat{\mathbf{x}} \times \mathbf{l}])/c\}\tag{21}$$

For definiteness let us assume that the instability occurs in the superconducting channel which is the most likely case for  $K_c > 1$ . Note that the duality property of the effective Lagrangian (10) under  $K \rightarrow 1/K$ ,  $V \leftrightarrow J$ ,  $\Theta \leftrightarrow \Phi$  means that all of the results in this and the next section are identical for the CDW channel.

In a Tomonaga-Luttinger liquid with the ultraviolet cut-off  $\Delta_s$  the static susceptibility for the operator with scaling dimension  $d$  is given by<sup>16</sup>

$$\chi^{(0)}(q) = \frac{2}{\Delta_s^2} \sin \pi d \left(\frac{2\pi T}{\Delta_s}\right)^{-2+2d} \Gamma^2(1-d) \left| \frac{\Gamma(d/2 + ivq/4\pi T)}{\Gamma(1-d/2 + ivq/4\pi T)} \right|^2.\tag{22}$$

where  $v$  is the velocity in the charge sector.

##### A. Zero magnetic field; the critical temperature and the vortex energy

Substituting (22) with  $q = 0$  into Eq.(19) we obtain

$$T_c = \frac{\Delta_s}{2\pi} \left( \frac{2Jz_{\perp}}{\Delta_s} \sin \pi d \frac{\Gamma^2(d/2)\Gamma^2(1-d)}{\Gamma^2(1-d/2)} \right)^{\frac{1}{2-2d}}.\tag{23}$$

Below the transition temperature the long-wavelength fluctuations of superconducting order parameter are three-dimensional. The amplitude fluctuations are, however, mostly one-dimensional and their spectral weight is concentrated above certain energy which plays a role of a pseudo-gap. The zero temperature value of the pseudo-gap can be

found from the mean-field theory combined with the exact results for the sine-Gordon model. In this approach one approximates the inter-chain interaction

$$J \sum_{\langle nm \rangle} \cos \beta(\phi_n - \phi_m) \quad (24)$$

( $\beta\phi = \sqrt{2\pi}\Theta$  and  $\beta^2 = 2\pi K_c^{-1}$ ) by

$$2\mu \cos \beta\phi \quad (25)$$

where

$$2\mu = Jz_{\perp} \Delta_s \langle \cos \beta\phi \rangle. \quad (26)$$

This expectation value is known exactly<sup>17</sup>:

$$\langle \cos \beta\phi \rangle = \frac{(1+\xi)\pi\Gamma(1-d/2)}{16 \sin \pi\xi \Gamma(d/2)} \left( \frac{\Gamma(\frac{1}{2} + \frac{\xi}{2})\Gamma(1-\frac{\xi}{2})}{4\sqrt{\pi}} \right)^{(d-2)} \left( 2 \sin \frac{\pi\xi}{2} \right)^d \left( \frac{M}{\Delta_s} \right)^d \quad (27)$$

where  $M$  is the soliton mass in the SG model, and is related to  $\mu$  by

$$\mu = \frac{\Gamma(d/2)}{\pi\Gamma(1-d/2)} \left( \frac{2\Gamma(\xi/2)}{\sqrt{\pi}\Gamma(\frac{1}{2} + \frac{\xi}{2})} \right)^{d-2} \left( \frac{M}{\Delta_s} \right)^{2-d} \Delta_s^2. \quad (28)$$

In all these equations,  $d = \beta^2/4\pi$  is the scaling dimension of the field  $e^{i\beta\phi}$ , and  $\xi = 1/(2-d)$ . These mean-field relations are solved to give

$$M = \Delta_s \left[ \frac{Jz_{\perp}}{\Delta_s} \frac{1}{2(d-2)} \tan \frac{\pi\xi}{2} \right]^{\frac{1}{2-2d}} \left[ \frac{\pi\Gamma(1-d/2)}{\Gamma(d/2)} \left( \frac{\Gamma(\frac{1}{2} + \frac{\xi}{2})\sqrt{\pi}}{2\Gamma(\xi/2)} \right)^{(d-2)} \right]^{\frac{1}{1-d}}. \quad (29)$$

The ratio  $T_c/M$  which is often considered in the theory of superconductivity is plotted as a function of  $d$  in figure 1. It's numerical value in certain limits is:

$$\frac{T_c}{M}(d=0) = \frac{\sqrt{2}}{8} \approx 0.177, \quad (30)$$

$$\frac{T_c}{M}(d=1/2) = \frac{3}{16} \frac{\sqrt{3\pi}(\Gamma(2/3)\Gamma(5/6))^3}{\Gamma(3/4)^8} \approx 0.404. \quad (31)$$

In the limit  $d \rightarrow 1$  which corresponds to weak coupling, our expressions for  $T_c$  and  $M$  diverge in this approximation. However their ratio can still be evaluated. Writing  $x = 1-d$  and expanding all the gamma functions as Taylor series in  $x$  gives us the BCS value

$$\frac{T_c}{M}(d \rightarrow 1) = \frac{1}{2\pi} \lim_{x \rightarrow 0} [1 + (\ln 2 + \gamma)x]^{\frac{1}{x}} = \frac{1}{\pi} e^{\gamma} \approx 0.567 \quad (32)$$

where  $\gamma \approx 0.57722$  is Euler's constant.

Notice that in comparing to experiments, one has to remember that  $M$  is not the single particle gap. Single particle spectroscopies such as basic tunneling would see a gap much closer to  $\Delta_s$ , the spin gap. To probe  $M$ , one would have to look at experiments involving pairs of electrons, such as Andreev tunneling. In the context of sine-Gordon model,  $M$  is the soliton mass. Solitons correspond to spatial changes in the superconducting phase  $\Theta$  and hence to vortices. Therefore  $M$  is the minimal energy necessary to create a vortex. It should also be noticed that at  $d < 1$  the sine-Gordon model has not only solitons, but bound states which, being neutral, should be interpreted as vortex-antivortex pairs. At  $d < 1/2$  the energy of the first bound state is smaller than the soliton. See Carlson *et al.*<sup>9</sup> for a nice discussion of the implications of having these two energy scales.

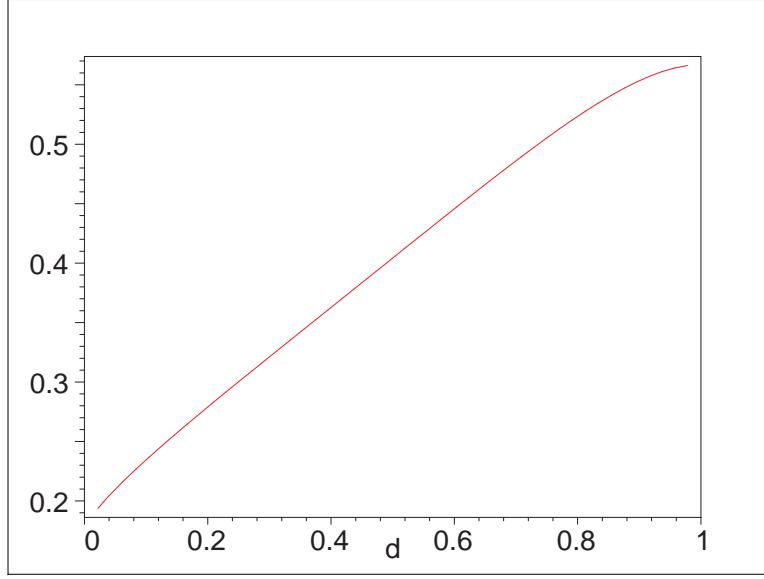


FIG. 1. A graph of  $T_c/M$  against  $d$ . The value  $d = 1$  corresponds to the BCS limit, decreasing  $d$  corresponds to increasing repulsion.

### B. Phase diagram in a magnetic field

To keep the calculations as simple as possible, let us consider the simplest possible situation when a given chain has four nearest neighbours with Josephson couplings  $J_z$  and  $J_y$  and the magnetic field lays in the  $yz$  plane. Combining Eq.(21) and Eq.(22) we obtain the equation for the critical temperature:

$$C \left( \frac{T_c}{T_c(0)} \right)^{(2-2d)} = J_z \left| \frac{\Gamma(d/2 + i\alpha b_z H_y/T_c)}{\Gamma(1-d/2 + i\alpha b_z H_y/T_c)} \right|^2 + J_y \left| \frac{\Gamma(d/2 + i\alpha b_y H_z/T_c)}{\Gamma(1-d/2 + i\alpha b_y H_z/T_c)} \right|^2$$

$$C = (J_z + J_y) \left| \frac{\Gamma(d/2)}{\Gamma(1-d/2)} \right|^2, \quad \alpha = ev/2\pi c \quad (33)$$

The solution of this equation describes several interesting effects.

- A possibility of a re-entrance behaviour.

Let us consider the case when in-plane interactions are isotropic:  $J_z = J_y, b_z = b_y$  and the magnetic field is directed at  $45^\circ$  angle  $H_z = H_y = H$ . This gives it the maximal power to suppress  $T_c$ . A numerical solution of Eq.(33) is plotted in figure 2 (a) for various values of the scaling dimension  $d$ . We see that there is a range of magnetic fields for which the superconductivity exists in an intermediate range of temperatures. To study the stability of these solutions one needs to have a good description of the ordered state in magnetic field, which we hope to obtain in the future.

At  $T_c \rightarrow 0$  Eq.(33) can be solved analytically which allows us to extract the value of critical field at  $T_c = 0$ :

$$H_c(0) = \frac{2\pi c}{e} \frac{T_c(0)}{bv} \left( \frac{\Gamma(1-d/2)}{\Gamma(d/2)} \right)^{1/(1-d)} \quad (34)$$

This is plotted in figure 2 (b) along with the numerical solution for  $H_c^{max}$ .

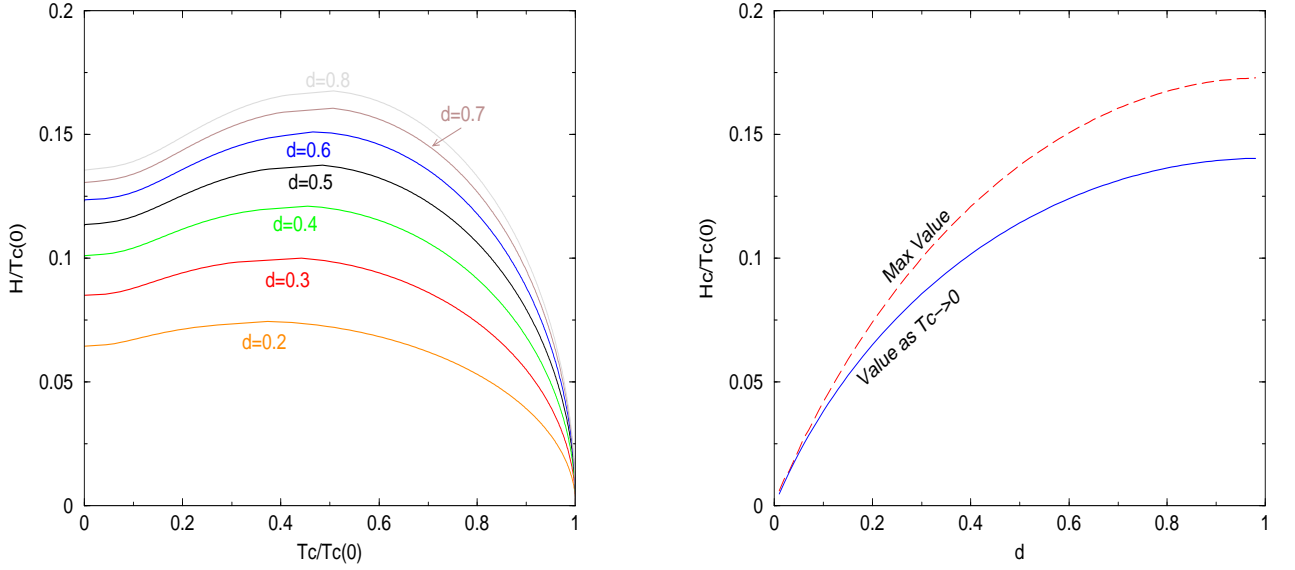


FIG. 2. (a) The critical temperature as a function of magnetic field for various values of  $d$ . (b) The critical magnetic field as a function of  $d$ . The magnetic field is measured in the units of  $2e\hbar v/c$ .

- Anisotropy of the phase diagram.

Another prediction following from Eq.(33) is an anisotropy of the phase diagram. This can be illustrated by an analytical solution for  $T_c \rightarrow 0$  case. Setting  $T_c \rightarrow 0$  Eq.(33) in we find

$$\frac{J_z}{(\alpha H_y b_z)^{2(1-d)}} + \frac{J_y}{(\alpha H_z b_y)^{2(1-d)}} = \frac{C}{[T_c(0)]^{2(1-d)}} \quad (35)$$

This is plotted in figure 3. We must be careful to remember however that this is a first order mean field calculation, and further corrections will give a critical flux in all directions, even when the field is pointing directly along one of the crystal axis.

- SC-CDW transition.

The validity of the above calculations is limited by the range of temperatures where the system is stable against CDW transition. Therefore, strictly speaking, before the  $T_c \rightarrow 0$  quantum critical point is reached the system will undergo a transition into a CDW state.

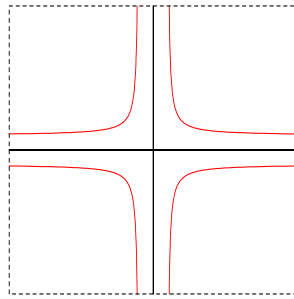


FIG. 3. Angular dependence of the critical magnetic field. This is plotted for  $d = 1/2$ . The graph is qualitatively similar for other values of  $d$ .

### C. The flux state

When a magnetic field penetrates into the material, the state becomes non-uniform. To see what kind of state we obtain let us consider again the simplest case of rectangular lattice with the magnetic field directed along the  $z$ -direction. We make a shift of the phase variable in Eq.(4):

$$\sqrt{2\pi}\Theta_n(x) \rightarrow \sqrt{2\pi}\Theta_n(x) + \frac{2ebxH}{c}N \left\{ \frac{n}{N} \right\} \quad (36)$$

where  $\{y\}$  means the fractional part of  $y$  and  $N$  is given by

$$N = [cM/2ebH] + 1 \quad (37)$$

with  $[y]$  meaning the integer part of  $y$  and  $M$  is the soliton mass. By making this transformation we remove the  $x$ -dependence from most of the oscillatory terms in Eq.(4) but add the terms

$$\frac{2ebH}{c\sqrt{2\pi}}N \left\{ \frac{n}{N} \right\} \partial_x \Theta_n. \quad (38)$$

The gradient term in the sine-Gordon model acts as a chemical potential; the variable shift is chosen in such a way that the chemical potential is always smaller than the soliton mass and therefore does not lead to incommensurability. The exception are modes with  $n = kN$  where  $k$  is an integer. For these modes the oscillatory term is not compensated by the shift (36). The corresponding contribution to the action is:

$$J : \cos[\sqrt{2\pi}\Theta_{kN} - \sqrt{2\pi}\Theta_{kN\pm 1} - (M + \delta h)x] : \quad (39)$$

where

$$\delta h = M(2eNbH/cM - 1) > 0 \quad (40)$$

In the mean field approximation we put  $\Theta_{kN\pm 1} = 0$  and obtain for  $kN$ -th chains the sine-Gordon model with a chemical potential which exceeds the critical value by the amount  $\delta h$ . Therefore these chains have a finite soliton density.

The magnetic field enters periodically separating the entire system into a sequence of superconducting stripes, as is shown on Figure 4 for the case  $N = 4$ . The period of this stripe picture is  $N$ . When the ratio  $2ebH/cM$  changes between  $1/N$  and  $1/(N-1)$ , the soliton density increases; when it reaches  $1/(N-1)$ , the period of the stripe structure changes by one. Again, this is easiest illustrated in pictorial form in figure 5.

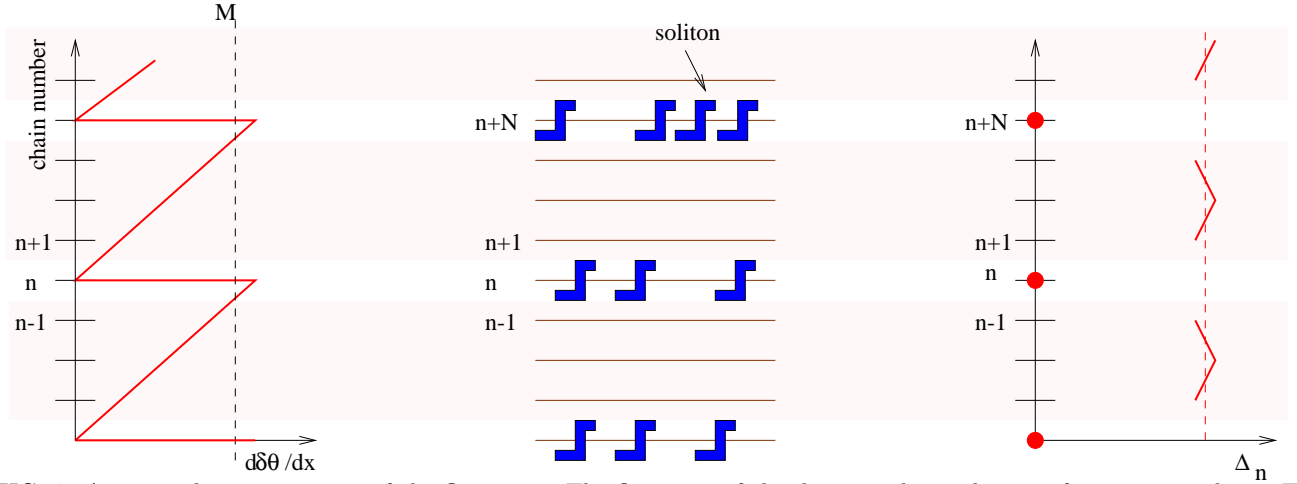


FIG. 4. A pictorial representation of the flux state. The first part of the diagram shows the transformation to theta. The gradient is proportional to the magnetic field. When this exceeds the soliton mass (in appropriate units), it must be set back to zero, but on these chains, solitons are formed destroying the superconductivity as shown in the second part of the figure. In the third part, the superconducting order parameter is plotted, which is zero on the non-superconducting stripes and slowly varying for the remaining chains. We see clearly here how the flux state in this strongly anisotropic material consists of superconducting 'stripes'.



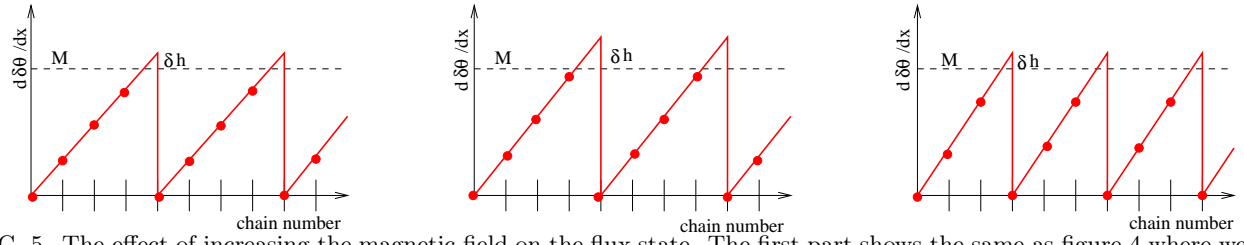


FIG. 5. The effect of increasing the magnetic field on the flux state. The first part shows the same as figure 4 where we have  $N = 4$ . The second part shows the effect of increasing  $H$  slightly;  $\delta h$  representing the soliton density increases in proportion, but nothing dramatic happens. Then in the third part, increasing  $H$  slightly more so that the chemical potential at  $n = 3$  would now be above the critical value, so the stripe period decreases to an  $N = 3$  state.

In describing the non-uniform state we neglected variations of the order parameter amplitude which, in principle, may affect the picture. To see that these variations are small let us consider the mean field equations for the non-uniform case. These equations are similar to those described in Section IV.A. The equations for the SC order parameter amplitude  $\langle \cos \beta \Theta_n \rangle$  for the quasi-2D geometry when  $J_z < J_y$  and the field is directed along the  $z$ -axis, have the following form:

$$\left( \frac{\Delta_n}{\Delta(0)} \right)^{2(1-d)/d} = \frac{1}{4} \left[ \frac{2J_z}{J_y} + \frac{\Delta_{n+1} + \Delta_{n-1}}{\Delta_n} \right], \quad n = 1 \dots N-1$$

$$\Delta_0 = \Delta_N = 0 \quad (41)$$

where  $\Delta(0)$  is the uniform value of the order parameter. This is demonstrated in the final part of figure 4.

Numerical solutions equation 41 show only a weak variation of  $\Delta_n$  away from the non-superconducting chains. In fact this equation over-estimates these differences as there will also be a coupling through these chains.

This weak variation is a good sign of the self-consistency of the above method as the soliton mass  $M$  depends on  $\Delta$  in the mean field picture. However as we can write  $\Delta_n = \bar{\Delta} + \delta_n$  where  $\delta_n \ll \bar{\Delta}$ , we can define  $M$  as that corresponding to an order parameter of  $\bar{\Delta}$  and then solve self-consistently.

The striped flux state opens the door to a variety of fascinating properties which we hope to study in detail at a later date.

## V. CORRECTIONS TO RPA

The analysis of the previous sections was based on RPA. Since in realistic situations the number of nearest neighbours is never large, it is important to check how robust RPA is. We will calculate corrections to RPA in the simplest case case of zero magnetic field. We shall also restrict ourselves to  $K_c = 1$  ( $d = 1/2$  for both interactions).

The basic RPA calculation involves only the stronger of the two interactions - for clarity let us again take this to be  $J$ . However as we mentioned before we would expect the presence of the other competing interaction of the same scaling dimension to also play a role. In particular we expect there to be a mode with a gap of  $J - V$ , seen in (18) and in the two chain model. This will be very important around the point  $V = J$  as it will become massless thereby increasing fluctuations and decreasing the transition temperature. This can be investigated by looking at the first correction to the RPA formula - figure 6(c).

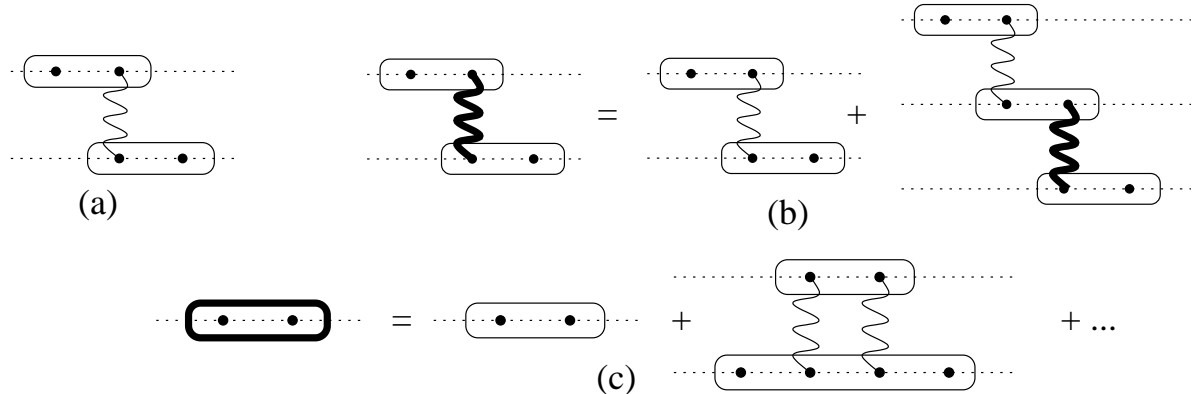


FIG. 6. (a) The basic RPA diagram, (b) The Dyson series for RPA, (c) The first correction term. In these diagrams, the dashed lines represent the 1D chains, the dots indicate vertex operators of  $\phi$  or  $\theta$  and the wiggly lines are the inter-chain interactions, and each diagram is an irreducible correlator.

In terms of the fields  $\phi$  and  $\theta$ , this diagram can be expressed as

$$\begin{aligned} \delta\chi = & V^2 z_{\perp} \left[ \langle e^{i\sqrt{2\pi}\phi(a)} e^{i\sqrt{2\pi}\theta(1)} e^{-i\sqrt{2\pi}\theta(2)} e^{-i\sqrt{2\pi}\phi(b)} \rangle - \langle e^{i\sqrt{2\pi}\phi(a)} e^{-i\sqrt{2\pi}\phi(b)} \rangle \langle e^{i\sqrt{2\pi}\theta(1)} e^{-i\sqrt{2\pi}\theta(2)} \rangle \right] \\ & \times \langle e^{-i\sqrt{2\pi}\theta(1)} e^{i\sqrt{2\pi}\theta(2)} \rangle \\ & + J^2 z_{\perp} \left[ \langle e^{i\sqrt{2\pi}\phi(a)} e^{i\sqrt{2\pi}\phi(1)} e^{-i\sqrt{2\pi}\phi(2)} e^{-i\sqrt{2\pi}\phi(b)} \rangle - \langle e^{i\sqrt{2\pi}\phi(a)} e^{-i\sqrt{2\pi}\phi(b)} \rangle \langle e^{i\sqrt{2\pi}\phi(1)} e^{-i\sqrt{2\pi}\phi(2)} \rangle \right] \\ & \times \langle e^{-i\sqrt{2\pi}\phi(1)} e^{i\sqrt{2\pi}\phi(2)} \rangle. \end{aligned} \quad (42)$$

The revised RPA equation for the transition temperature is

$$1 = \frac{J z_{\perp}}{T_c} \left[ A_0^J + A_1^J \frac{J^2 z_{\perp}}{T_c^2} + A_1^V \frac{V^2 z_{\perp}}{T_c^2} \right] \quad (43)$$

where the coefficients are given by

$$A_0^J = \frac{1}{\pi} \int_0^{\pi} d\tau \int_{-\infty}^{\infty} dx \frac{1}{|\sinh(x + i\tau)|} = \frac{1}{2\pi} B^2(1/4, 1/2) \quad (44)$$

$$\begin{aligned} A_1^J = & \frac{1}{\pi^3} \int_0^{\pi} d\tau_1 d\tau_2 d\tau_b \int_{-\infty}^{\infty} dx_1 dx_2 dx_b \frac{1}{|\sinh(x_b + i\tau_b)|} \frac{1}{|\sinh(x_{12} + i\tau_{12})|^2} \\ & \times \left[ \frac{|\sinh(x_1 + i\tau_1)| |\sinh(x_{b2} + i\tau_{b2})|}{|\sinh(x_2 + i\tau_2)| |\sinh(x_{b1} + i\tau_{b1})|} - 1 \right] \end{aligned} \quad (45)$$

$$\begin{aligned} A_1^V = & \frac{1}{\pi^3} \int_0^{\pi} d\tau_1 d\tau_2 d\tau_b \int_{-\infty}^{\infty} dx_1 dx_2 dx_b \frac{1}{|\sinh(x_b + i\tau_b)|} \frac{1}{|\sinh(x_{12} + i\tau_{12})|^2} \\ & \times \left[ \left( \frac{\sinh(x_1 + i\tau_1) \sinh(x_2 - i\tau_2) \sinh(x_{b2} + i\tau_{b2}) \sinh(x_{b1} - i\tau_{b1})}{\sinh(x_1 - i\tau_1) \sinh(x_2 + i\tau_2) \sinh(x_{b2} - i\tau_{b2}) \sinh(x_{b1} + i\tau_{b1})} \right)^{1/2} - 1 \right] \end{aligned} \quad (46)$$

with  $x_{12} = x_2 - x_1$  and so on.

The integrals are evaluated numerically by Monte-Carlo techniques,<sup>18</sup> with values calculated over finite volumes then scaled to infinity. The results are

$$\begin{aligned} A_0^J &= 4.377, \\ A_1^J &= 34.81 \pm 0.02, \\ A_1^V &= -33.01 \pm 0.02. \end{aligned} \quad (47)$$

Hence the correction to the transition temperature is

$$\frac{T_c}{A_0^J J z_{\perp}} \approx 1 + \frac{1}{z_{\perp}} \left[ 0.42 - 0.40 \left( \frac{V}{J} \right)^2 \right]. \quad (48)$$

This expression is valid for  $J > V$ . If  $V > J$ , the expression is exactly the same, but with  $V \leftrightarrow J$ . This is plotted in figure 7 and gives a dip near the critical point as expected.

It is interesting to note that in the absence of the second interaction term, ie  $V = 0$ , these correction raise the transition temperature above the RPA value. This differs from models of coupled spin chains where RPA tends to overestimate the transition temperature.<sup>7,8</sup>

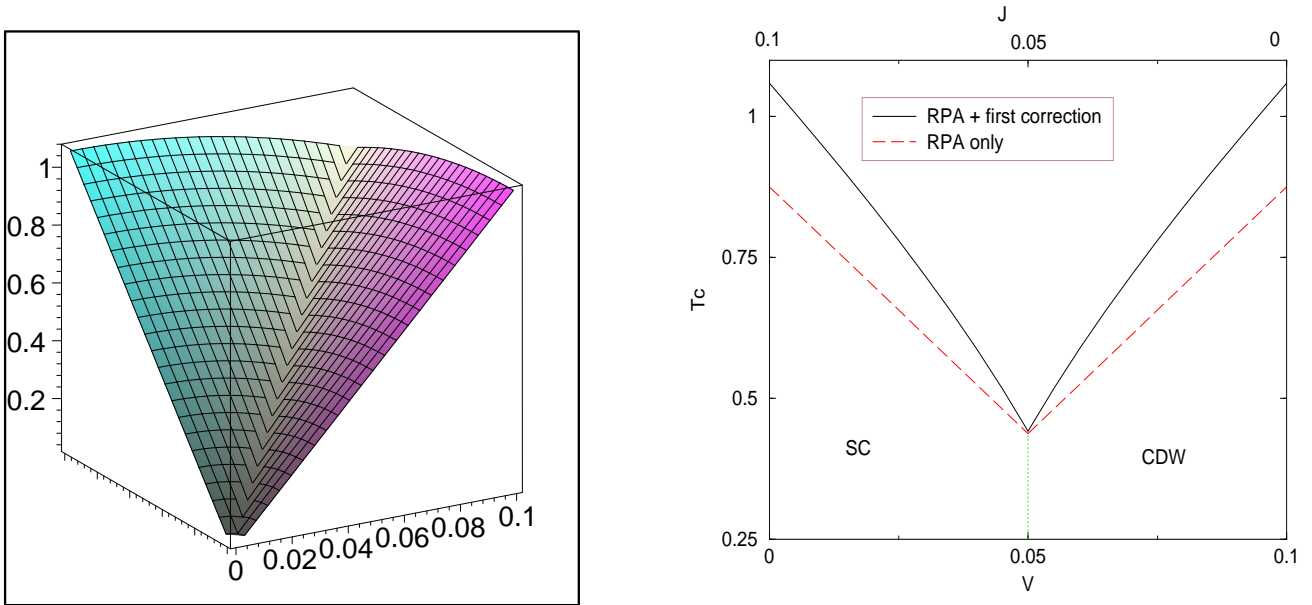


FIG. 7. (a) A plot of  $T_c$  against  $V$  and  $J$ , (b) A cross section of  $T_c$  against  $V$  along the line  $V + J = 0.1$ . In these plots, we have taken  $z_\perp = 2$  to allow these corrections to be clearly seen, although for this approach to be valid, we require  $z_\perp \geq 3$ .

## VI. A WORD ABOUT TWO DIMENSIONS

In two dimensions the RPA approach in the previous two sections must break down completely, as spontaneous symmetry breaking is forbidden by the Mermin-Wagner theorem. We can see how this comes about by looking at figure 6(c). The correction we looked at involved only bare couplings to the bare correlation function. The process of making these lines 'thick' involves much numerical complication and gives rise to only small corrections in three or higher dimensions.<sup>7</sup> However in two dimensions, these corrections have infra-red divergences and drive the transition temperature back down to 0.

Nevertheless we still get a transition in two dimensions: it is of the Kosterlitz-Thouless<sup>19,20</sup> type. Let's look closer at Coulomb coupling in two dimensions. The Lagrangian for the coupled chains can be written

$$\mathcal{L} = \sum_i \left\{ \frac{1}{2} (\partial_\mu \phi_i)^2 - J \cos[\beta(\phi_i - \phi_{i+1})] \right\}. \quad (49)$$

By making the approximation

$$-\cos \phi = \frac{\phi^2}{2} \langle \cos \phi \rangle \quad (50)$$

which comes from the diagrammatic expansion, we can write this as

$$\mathcal{L} = \sum_i \left\{ \frac{1}{2} (\partial_\mu \phi_i)^2 + \tilde{J} (\phi_i - \phi_{i+1})^2 \right\} \quad (51)$$

with the self-consistent relation

$$\begin{aligned} \tilde{J} &= J \beta^2 \langle \cos \beta(\phi_i - \phi_{i+1}) \rangle \\ &= J \beta^2 \exp \left\{ -\beta^2 T \sum_n \int \frac{dq_\perp}{2\pi} \frac{dq_\parallel}{2\pi} \frac{1 - \cos q_\perp}{\omega_n^2 + q_\parallel^2 + 4\tilde{J} \sin^2(q_\perp/2)} \right\}. \end{aligned} \quad (52)$$

At  $T = 0$  this relation becomes

$$\begin{aligned}
\tilde{J} &= J\beta^2 \exp\left(-\frac{\beta^2}{2\pi} \ln \frac{\Delta_s}{\sqrt{2\tilde{J}}}\right) \\
&= J\beta^2 \left(\frac{\tilde{J}}{\Delta_s}\right)^d
\end{aligned} \tag{53}$$

where  $d = \beta^2/4\pi$  as before. As  $T$  increases, the self-consistent value of  $\tilde{J}$  will decrease, but for an estimate of the behaviour of the transition temperature this relation will suffice.

The Kosterlitz-Thouless transition temperature<sup>1,20</sup>  $T_{KT} \sim \sqrt{\tilde{J}}$  hence we have

$$T_{KT} \sim \Delta_s \left(\frac{J}{\Delta_s}\right)^{\frac{1}{2-2d}} \tag{54}$$

giving the same order of magnitude as the ordering temperature in higher dimensions (23).

Hence in two dimensions, although the nature of the transition is different, the energy scales involved are the same as in higher dimensions. The only major difference occurs when approaching the SU(2) critical point where the presence of a non-Abelian symmetry in two dimensions means that the transition temperature will drop to zero at this point. The qualitative phase diagram in two dimensions is shown in figure 8.

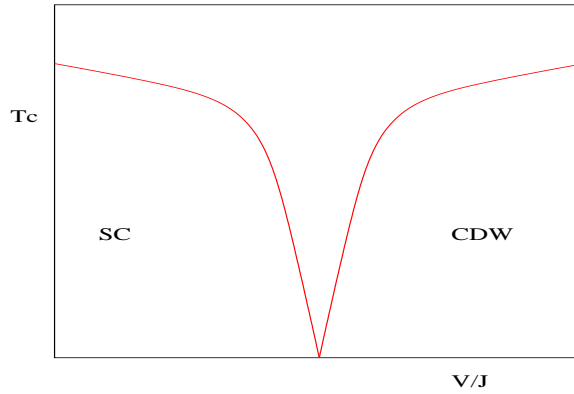


FIG. 8. The modified phase diagram for our model in two dimensions

## VII. AN EXAMPLE EXPERIMENTAL SYSTEMS

The class of materials  $\text{Sr}_{12-x}\text{Ca}_x\text{Cu}_{24}\text{O}_{41}$  are built up from alternating layers of weakly coupled  $\text{CuO}_2$  chains and  $\text{Cu}_2\text{O}_3$  two-leg ladders. The material shows a spin gap in both of these one-dimensional units,<sup>21</sup> making it a prime candidate for application of our model. Our theory is still valid even if the superconductivity originates from the ladders.

For  $x \geq 11.5$ , these materials show superconductivity under pressure,<sup>22,23</sup> and NMR studies also indicate possible charge ordering at low temperature and ambient pressure.<sup>21</sup> One of the most interesting measurements however is the resistivity. For  $\text{Sr}_{2.5}\text{Ca}_{11.5}\text{Cu}_{24}\text{O}_{41}$  these measurements<sup>23</sup> show a number of features:

- Below about 4 GPa pressure, the temperature dependence of the resistivity perpendicular and parallel to the ladders is different. This indicates that different mechanisms are governing the transport in these two directions, consistent with the spin-gap concept. Above 4 GPa the temperature dependence of the resistivity anisotropy becomes weak, which indicates that single particle hopping between ladders is now possible, i.e. the spin gap has vanished and we have a crossover to a conventional two-dimensional metallic behaviour. This is consistent with the pressure dependence of the spin gap observed in recent NMR experiments.<sup>24</sup>
- At sufficiently high temperatures, coherent inter-ladder charge dynamics is also seen. The temperature where this occurs is consistent with the NMR determinations of the spin gap, so we may conclude that the transport properties of this material are indeed governed by weakly interacting one-dimensional spin-gapped units.

In figure 9 a qualitative phase diagram of this material is shown.<sup>24</sup> This is explained in terms of our model. If we take  $K_s \approx 1$  we have

$$\begin{aligned} J_{\text{eff}} &\sim t^2/\Delta_s, \\ V_{\text{eff}} &\sim V_0(\Delta_s/\Lambda). \end{aligned} \quad (55)$$

The increase of spin gap leads to decrease in the effective inter-ladder Josephson coupling. Hence eventually the inter-ladder Coulomb interaction takes over and the superconductivity disappears. In quasi-two-dimensional the SC and CDW regions of the phase diagram are separated by the quantum critical point, as described in Section VI.

It would be interesting for this material to measure the charge gap in the superconducting region. This may be achieved via optical conductivity measurements. For the Luttinger liquid parameter  $K_c \approx 1$ , our model then predicts the ratio  $T_c/\Delta_c$  to be the non-BCS value of order of 0.4.

Also in this material,  $T_c$  is very small in comparison to the Fermi energy  $v/a$ , so the magnetic field effects on the superconducting state should be strong. This would be another interesting experiment to perform.

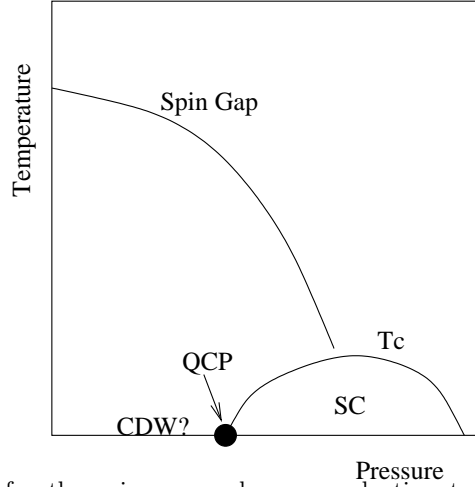


FIG. 9. Qualitative phase diagram for the spin gap and superconducting transition temperature against pressure in  $\text{Sr}_2\text{Ca}_{12}\text{Cu}_{24}\text{O}_{41}$

## VIII. CONCLUSION

We have discussed a model with the following hierarchy of energy scales:

1. The highest energy scale is the spin gap  $\Delta_s$ . Below  $\Delta_s$  the system is described by competing CDW and SC fluctuations.
2. There is a transition temperature at which either  $\langle \cos \sqrt{2\pi}\Theta \rangle$  or  $\langle \cos \sqrt{2\pi}\Phi \rangle$  are formed. According to the mean field calculation, these order parameters cannot be formed simultaneously. Thus we are either in CDW or SC phase, but the temperature of their formation goes smoothly through the point  $V = J$ .
3. There is a third energy scale associated with the gap for another mode which becomes soft at the critical point. This mode is not seen in the first order RPA calculations, but its effects can be noted by looking at the first correction to RPA.

Within the RPA approximation we calculated the transition temperature for general  $K_c$ . We calculated the ratio  $T_c/M$  where  $M$  is the zero temperature gap in the charge sector. We saw that this decreases below the BCS value as the coupling strength is increased. We also looked at the properties of our model in a magnetic field, noting in particular the extreme anisotropy of the phase diagram, and the existence of a flux state consisting of superconducting stripes. This is a topic for further investigation.

We then went on to calculate the first corrections to  $T_c$  in the vicinity of the critical point which is decreased because of the interplay between the two interactions. We also showed that in two dimensions where RPA breaks down completely, we get a transition of the Kosterlitz-Thouless type which has the same energy scales as the ordering

transition in higher dimensions. We also showed that the compound  $\text{Sr}_2\text{Ca}_{12}\text{Cu}_{24}\text{O}_{41}$  is likely to be described by our model and on this basis made further predictions about its properties and suggested that optical conductivity experiments should be done on such a material.

S.T.C. acknowledges many useful discussions with Ralph Werner. A.M.T. is grateful to Marc Bocquet for giving him his preprint before publication. The work is supported by the US DOE under contract number DE-AC02-98 CH 10886 and EPSRC grant number 99307266.

## APPENDIX A: ESTIMATE OF THE EFFECTIVE COUPLINGS

The easiest case is that of the Coulomb coupling. In the bare system, we have a term

$$\mathcal{H}_{\text{coulomb}} = \frac{V_0}{a_0} \sum_{n \neq m} \rho_n(x) \rho_m(x) \quad (\text{A1})$$

with  $\rho(x)$  the charge density on each chain, and  $V_0$  is the strength of the inter-chain Coulomb coupling. When we open a spin gap, two things happen to this expression. Firstly, anything involving the spin field is replaced by its average value  $\langle \cos(\sqrt{2\pi}\Phi_s) \rangle \sim (\Delta_s/a_0^{-1})^{K_s/2}$ . Secondly, the cut-off in the normal ordering of the charge sector is changed from  $a_0^{-1}$  to  $\Delta_s$ . This gives an extra factor of  $(\Delta_s/a_0^{-1})^{K_c/2}$  for each operator. Overall, we generate an effective interaction

$$\mathcal{H}_{\text{cdw}} = \frac{1}{2} \frac{V_{\text{eff}}}{\Delta_s^{-1}} \sum_{n \neq m} : \cos[\sqrt{2\pi}(\Phi_n - \Phi_m)] : \quad (\text{A2})$$

where

$$V_{\text{eff}} \sim \left( \frac{\Delta_s}{a_0^{-1}} \right)^{K_s + K_c - 1} V_0. \quad (\text{A3})$$

In this paper, we will be keeping  $K_s \approx 1$ .

In the case of the effective Josephson coupling, we start from a single particle hopping term in our bare Hamiltonian density

$$\mathcal{H}_{\text{hopping}} = \frac{t}{2a_0} \sum_{n \neq m} \{ R_n^\dagger R_m + L_n^\dagger L_m \}. \quad (\text{A4})$$

After opening the spin-gap, the effective Hamiltonian density only involves pair hopping:

$$\mathcal{H}_{\text{sc}} = \frac{1}{2\Delta_s^{-1}} J_{\text{eff}} \sum_{n \neq m} : \cos[\sqrt{2\pi}(\Theta_n - \Theta_m)] :. \quad (\text{A5})$$

These are virtual processes involving an intermediate energy  $\Delta_s$ , hence the  $J_{\text{eff}}$  will have a factor  $t^2/\Delta_s$ . We must also remember to change the cut-off in the normal ordering, so the overall expression is

$$J_{\text{eff}} \sim \left( \frac{\Delta_s}{a_0^{-1}} \right)^{1/K_c - 1} \frac{t^2}{\Delta_s} \quad (\text{A6})$$

## APPENDIX B: MEAN FIELD SOLUTION FOR MANY CHAINS

In the mean field approximation, the interaction term is

$$\begin{aligned} \mathcal{L}_{\text{int}} &= \sum_m \{ V \cos[\sqrt{2\pi}(\Phi_n - \Phi_m)] + J \cos[\sqrt{2\pi}(\Theta_n - \Theta_m)] \} \\ &\approx z_\perp V \langle \cos[\sqrt{2\pi}\Phi] \rangle \cos[\sqrt{2\pi}\Phi_n] + z_\perp J \langle \sin[\sqrt{2\pi}\Theta] \rangle \sin[\sqrt{2\pi}\Theta_n]. \end{aligned} \quad (\text{B1})$$

This can be written as

$$\mathcal{L}_{\text{int}} = \sqrt{A^2 + B^2} \text{Tr}[(\cos \gamma I + i\sigma^1 \sin \gamma)g + c.c],$$

$$A = Vz_{\perp} \langle \cos[\sqrt{2\pi}\Phi] \rangle, \quad B = Jz_{\perp} \langle \sin[\sqrt{2\pi}\Theta] \rangle, \quad \tan \gamma = \frac{B}{A} \quad (\text{B2})$$

The constant matrix can be removed by the redefinition of  $g$ . After that it becomes evident that the free energy depends only on  $R^2 = A^2 + B^2$ . The mean field equations are

$$A = -Vz_{\perp} \frac{\partial F}{\partial A} = -Vz_{\perp} \frac{A}{R} \frac{\partial F}{\partial R},$$

$$B = -Jz_{\perp} \frac{\partial F}{\partial B} = -Jz_{\perp} \frac{B}{R} \frac{\partial F}{\partial R} \quad (\text{B3})$$

From this it is clear that the only case where both  $A$  and  $B$  are simultaneously non-zero is  $V = J$ .

- <sup>1</sup> A.O.Gogolin, A.A.Nersesyan, and A.M.Tsvetik, *Bosonization and Strongly Correlated Systems* (Cambridge University Press, Cambridge, UK, 1998).
- <sup>2</sup> V.J.Emery, in *Highly Conducting One-Dimensional Solids*, edited by R. J.T.Devreese and V. Doren (Plenum, New York, 1979), p. 327.
- <sup>3</sup> A.M.Finkel'stein and S.A.Brazovskiy, J. Phys. C **14**, 847 (1981).
- <sup>4</sup> H.Schulz, Phys. Rev. Lett. **77**, 2790 (1996).
- <sup>5</sup> F.H.L.Essler, A.M.Tsvetik, and G.Delfino, Phys. Rev. B **56**, 11001 (1997).
- <sup>6</sup> M.Bocquet, F.H.L.Essler, A.M.Tsvetik, and A.O.Gogolin, Phys. Rev. B **64**, 94425 (2001).
- <sup>7</sup> V.Y.Irkhin and A.A.Katanin, Phys. Rev. B **61**, 6757 (2000).
- <sup>8</sup> M.Bocquet, cond-mat/0110429 (2001).
- <sup>9</sup> E.W.Carlson, D.Orgad, S.A.Kivelson, and V.J.Emery, Phys. Rev. B **62**, 3422 (2000).
- <sup>10</sup> V.J.Emery, S.A.Kivelson, and J.M.Tranquada, Proc. Natl. Acad. Sci. **96**, 8814 (1999).
- <sup>11</sup> V.J.Emery, S.A.Kivelson, and O.Zachar, Phys. Rev. B **59**, 15641 (1999).
- <sup>12</sup> V.J.Emery and S.A.Kivelson, Nature **397**, 410 (1995).
- <sup>13</sup> E.Witten, Commun. Math. Phys. **92**, 455 (1984).
- <sup>14</sup> C.Itzykson and J-M.Drouffe, *Statistical Field Theory* (Cambridge University Press, Cambridge, UK, 1989), Vol. 2.
- <sup>15</sup> D.G.Shelton, A.A.Nersesyan, and A.M.Tsvetik, Phys. Rev. B **53**, 8521 (1996).
- <sup>16</sup> H.J.Schulz and C.Bourbonnais, Phys. Rev. B **27**, 5856 (1983).
- <sup>17</sup> S.Lukyanov and A.B.Zamolodchikov, Nucl. Phys. B **493**, 571 (1996).
- <sup>18</sup> W.H.Press, S.A.Teukolsky, W.T.Vetterling, and B.P.Flannery, *Numerical Recipes in C* (Cambridge University Press, Cambridge, UK, 1992).
- <sup>19</sup> V.L.Berezinskii, Soviet Physics JETP **32**, 493 (1970).
- <sup>20</sup> J.M.Kosterlitz and D.J.Thouless, J. Phys. C **6**, 1181 (1973).
- <sup>21</sup> M.Takigawa, N.Motoyama, H.Eisaki, and S.Uchida, Phys. Rev. B **57**, 1124 (1998).
- <sup>22</sup> M. Uehara *et al.*, Phys. Soc. Jpn. **65**, 2764 (1996).
- <sup>23</sup> T.Nagata *et al.*, Phys. Rev. Lett. **81**, 1090 (1998).
- <sup>24</sup> Y.Piskunov *et al.*, cond-mat/0110559 (2001).